Supplemental Material: (Omura *et al*; Robust axonal regeneration occurs in the injured CAST/Ei mouse central nervous system)

Supplemental Methods (Related to Methods)**:**

Primary dissociated DRG cultures: For growth on laminin, 1,500 cells were plated on 8-well chamber slide dish and cultured for 17 hours. Three independent experiments are performed.

DRG Explant cultures: Either naïve or pre-conditioned L4/L5 DRGs 8 week old mice were dissected free of spinal and peripheral roots and plated onto 8-well chamber slide dish (Lab-Tek) coated with thin layer of Matrigel (BD Biosciences). DRG explants were cultured in full Neurobasal media with B27 supplement for 48 hours. Non-overlapping quadrant pictures were taken at low power (4×) for analysis. The total length of neurite attached to the DRG was measured using WIS-NeuroMath.

Sciatic nerve pinch test: Three days after sciatic nerve crush, the left sciatic nerve exposed. Then under light anesthesia (0.75 to 1% isoflurane), starting distally, a series of pinches using a fine smooth forceps was delivered to the sciatic nerve moving proximally toward the injury site. The distance (mm) was recorded from the injury site to the most distal point on the nerve where the mouse produced a reflex withdrawal when pinched. For preconditioned pinch test, the second crush was performed 5 days after the first crush then assayed after 3 days. The site of sciatic nerve crush was marked with a 10-0 epineural suture. As in (Ma et al., 2011).

Assessment of sensory recovery using a pinprick assay: Eight week old C57BL/6J and CAST/EiJ mice were placed on wire mesh cages, habituated for three sessions the week before sciatic nerve crush or transection and tested on postoperative days accordingly. After a 30 minutes habituation period, an Austerlitz insect pin (size: 000) (FST) was gently applied to the plantar surface of the paw without moving the paw or penetrating the skin. The most lateral part of the plantar surface of the hindpaw (sensory field of the sciatic nerve) was divided into 5 areas (see Figure 5A). The pinprick was applied (twice) from the most lateral toe (area 5) to the heel (area 1). A response was considered positive when the animal briskly removed its paw, and the mouse was graded 1 for this area, and then tested for the next one. If none of the applications elicited a positive response, the overall grade was 0. In that case, the saphenous territory of the same paw was tested as a positive control, which always elicited a positive response. Scoring was done blinded to the surgery. As in (Ma et al., 2011).

Spinal cord staining: Spinal cords were embedded in OCT compound (Sakura Finetek), and serial 20µm sections were cut in the sagittal plane. Transverse sections of the spinal cord (3mm caudal and 5 mm rostral to the lesion) were taken to confirm the completeness of the lesion and to quantify tracing efficiency among experimental groups. Mice with incomplete lesions were excluded. For C57BL/6 naïve n=4, C57BL/6 conditioned n=5, CAST/Ei naïve n=6, CAST/Ei conditioned n=7. Staining for anti GFAP (Millipore) at 1:500 dilution were performed following standard protocols. Micro-Ruby signals were amplified using TSA signal amplification kit (PerkinElmer). As in (Puttagunta et al., 2014).

Dorsal column injury longest axon quantification: For the quantification of dorsal column injury model, the retrogradely labeled axons by micro-Ruby tracer were imaged by Nikon Eclipse 80i microscope and the longest regenerating fibers traced per cord by micro-Ruby tracer and were measured using Image J (NIH).

Optic nerve injury: Adult mice were anesthetized with a combination of ketamine (1 mg/10 g body weight) and xylazine (0.1 mg/10 g body weight) given i.p. A conjunctival incision was made over the dorsal aspect of eye, which is then gently rotated downward in the orbit. The orbital muscles were separated to expose the optic nerve at its exit from the globe, which is then crushed for 5 seconds with jewelers' forceps near the back of the eye (within 0.5 mm). As in (Yin et al., 2006)

Mouse model of stroke: Animal procedures were performed in accordance with the US National Institutes of Health Animal Protection Guidelines and the University of California Los Angeles Chancellor's Animal Research Committee. Focal cortical strokes on adult C57BL/6 and CAST/Ei male mice weighing 20–25 g (2–4 months old, Jackson Laboratories) were produced by photothrombosis as previously described (Clarkson et al., 2013; Overman et al., 2012). Briefly, under isofurane anesthesia, mice were placed in a stereotactic apparatus with the skull exposed through a midline incision, cleared of connective tissue, and dried. A cold light source (KL1500 LCD; Carl Zeiss MicroImaging, Inc.) attached to a 40x objective, giving a 2-mm diameter illumination, was positioned 1.5 mm lateral from the bregma used to produce a 2-mm diameter focal stroke upon light illumination. After 5 min, the brain was illuminated through the intact skull for 15 min. The mice were then sutured along the scalp, removed from the stereotactic frame (Model 900, David Kopf Instruments), and allowed to recover. Body temperature was maintained at 37.0 °C with a heating pad throughout the operation. Control animals received no stroke. At day 21 after stroke each mouse received an injection of 300 nl of 10% BDA (Sigma) into the forelimb motor cortex (A/P, 1.5 mm; M/L, 1.75 mm; D/V, 0.75 mm). At 28 d after stroke, mice were perfused with paraformaldehyde and the cortex removed, flattened and sliced to 40 µm tangentially (Clarkson et al., 2013; Li et al., 2010; Overman et al., 2012).

Quantitative cortical mapping of axonal sprouting: Axonal sprouting was quantified by digitally marking each BDA positive process in the cortex with a digitizing microscope system (Leica Microsystems, Ludl Electronic Products) and analysis program (Stereoinvesigator, MBF Biosciences). A BDA-labeled process was plotted irrespective of its cellular position as an axon shaft, pre-terminal or terminal axon field. This allowed each tangential map of axonal connections to contain an unbiased picture of the entire projection zone and trajectory of projections from forelimb motor cortex in each case. BDA-positive processes were marked in x,y coordinates relative to the center of the injection site by an observer blind to the treatment conditions. This process generates an x,y plot of the location of all labeled axons in each brain section. The x,y axonal plots of each brain from each experimental group were registered to the injection site and co- registered with functionally relevant anatomical regions, produced by the staining of the mouse somatosensory body map in cytochrome oxidase. Custom software (Li et al., 2010; Overman et al., 2012) produces quantitative connectional maps that consist of pixels, with the number of axons in each pixel mapped in register with anatomical brain structures. Polar plots were constructed with the x,y position of each BDA-labeled element plotted in relation to the tracer injection in forelimb motor cortex as the origin. This polar mapping shows both location and direction of axonal label. Surface maps and polar maps analyzed for statistically significant differences in connectional profiles between treatment groups (see below). In a separate quantification method, the number of axons within the ipso-hemisphere was counted a linear construct from the center of the injection site through the ipsilateral cortical hemisphere.

Stroke infarct volume was calculated by multiplying lesion area by the thickness of each section plus the distance between sections and then added with these measurements from the total area of the motor system projections for each brain was calculated from the 70% boundary of labeled axons in each arc of the polar plot of axonal label for that animal. BDA injection volume was measured by calculating the average injection core volume for each treatment group. The average BDA injection area in each section, determined by outlining the limit of extracellular tracer deposition, was multiplied by the sum of the thickness of the section and then summed for all sections in the series. Anterior–posterior and medial–lateral BDA injection location was analyzed by measuring the distance from the center of the injection site to the rostral edge of the tissue and the midline of the cortex, respectively.

The size and location of each BDA injection and stroke size did not vary significantly across individuals or by treatment condition.

Statistical analysis (Stroke): For quantitative connectional maps, three statistical analysis paradigms were used (Clarkson et al., 2013; Li et al., 2010; Overman et al., 2012). First, scatter plots were analyzed using Hotelling's T^2 test for spatial correlation. For data with a common covariance matrix, such as the map of axonal position in tangential cortical sections, Hotelling's T^2 method tests the hypothesis of multivariate mean equality: that the means for the set outcome variable (axonal location for each individual, averaged by experimental condition) are equivalent across groups. The T statistic is the analog of Student's two-group t-statistic for testing equality of group means for a single outcome variable. P-values were computed without Gaussian assumptions by means of a bootstrap 250 µm was applied around the injection site to account for the uniformity of the injection site itself and immediately adjacent BDA labeling across groups, regardless of sprouting pattern. Second, polar statistics tested for differences in distribution of axonal projection patterns across treatment groups. For each treatment condition, the x, y coordinate of every BDA-positive process was converted to an equivalent polar coordinate (r,) relative to the injection site as center. The location of each process was transferred to common polar space and a mean projection vector was computed for each treatment group. Differences in mean projection vectors between groups were analyzed using Watson's nonparametric two-sample U^2 test (Li et al., 2010; Overman et al., 2012). Third, the total areal extend of axonal label was computed for each animal using the polar plots. Data was tested with a paired, two-tailed students T test.

RNAseq Screen Protocol: DRG axonal length in a CNS inhibitory environment classifies the strains assayed into three groups: the C57BL/6 strain shows little if any growth pre- or post-preconditioning; the CAST/Ei strain shows very strong growth post pre-conditioning, whereas the other strains tested (including the DBA/2) display a low level but intermediate CNS growth post pre-conditioning. We searched for genes whose expression is significantly increased after pre-conditioning injury in the DBA/2 and CAST/Ei strain. To specifically select for genes responsible for the medium-low to strong growth phenotype, we removed any genes that showed significant regulation across the C57BL/6 naïve, C57BL/6 pre-conditioned, DBA/2 naïve and the CAST/Ei naïve phenotypes. From this list, we removed any gene with a fold change in CAST/Ei and DBA/2 strains that was less than the maximum fold change observed in the C57BL/6 strain after injury. In addition, to be consistent with the growth phenotype identified, we retained only genes whose fold change after injury is greater in the CAST/Ei strain than in the DBA/2. This resulted in a list of 16 genes for which we plotted the expression fold change (compared to the C57BL/6 naive expression level) across all 6 conditions (Figure 5c-e).

Immunohistochemistry: After perfusion with saline and 4% PFA, neuronal tissues were dissected and post-fixed for 2 hours then kept in 30% sucrose. DRG sections were cut at 10µm then stained for anti INHBA antibody (Sigma, HPA020031), anti-Acvr2A (Abcam, #ab96793) and phosho-Smad 2/3 (Cell Signaling, #8828).

In situ hybridization: Tissue was rapidly removed, embedded in Tissue-Tek OCT and frozen. Sections were cut serially at 10µm, and in situ hybridization performed using digoxygenin-labeled antisense and sense riboprobes. As in (Griffin et al., 2007).

Rat retinal ganglia culture: Adult rat retinal cultures were prepared as described (Yin et al., 2003). Briefly, RGCs were retrogradely labeled by injecting Fluorogold into the superior colliculus. One week later, the rat received a priming treatment: 6.4µg of zymosan intraocular injection immediately after the optic nerve crush. Three days after the priming, retinas were dissected, dissociated, and the cells plated in defined, serum-free medium in the presence of 10ng/ml of recombinant Activin A, B and AB (R&D, USA) or PBS containing 0.1% BSA. Axon growth (% RGCs extending axons <30 µm in length) was evaluated after 3 days in quadruplicate samples in a blinded fashion. As in (Yin et al., 2003).

Supplemental Figure Legends:

Suppl Figure 1: Axonal growth in a permissive peripheral environment (Related to Figure 1) **A:** Photomicrographs of dissociated naïve DRG neurons grown on the permissive substrate laminin for 17 hours. Scale, 100 µm. **B:** Temporal change in total axonal growth on laminin of naïve and preconditioned C57BL/6 and CAST/Ei DRG neurons at early time points. **C:** Representative photomicrographs of C57BL/6 and CAST/Ei DRG explant cultures when grown on the permissive substrate Matrigel for 48 hours. Scale, 100 µm **D:** Axonal growth quantification for Matrigel growth experiment. **E-F:** Peripheral axonal growth *in vivo* assayed using the sciatic nerve pinch test (E) and foot pad pinprick assay (F) in naïve and preconditioned C57BL/6 and CAST/Ei animals. Statistical analysis of B: Two-way ANOVA; post-hoc Sidak's, **p<0.001. For D and E: Student's t-test, two-tailed * p<0.05; ** p<0.01; **** p<0.0001.

Suppl Figure 2: C57 axonal regeneration in the adult spinal cord (Related to Figure 2)**:** Regeneration of central axons of pre-conditioned DRG neurons rostral to a dorsal column injury. A small level of growth is present in C57BL/6 mice, **A:** Second animal example relative to first shown in Figure 2. **B:** Third C57BL/6 injured spinal cord. Arrows identify retrogradely labeled axons from the PNS. Asterisk indicates the sight of injury.

Suppl Figure 3: CAST axonal regeneration in the adult spinal cord (Related to Figure 2)**:** Regeneration of central axons of pre-conditioned DRG neurons rostral to a dorsal column injury. A small level of growth is present in CAST/Ei mice, **A:** Second animal example relative to first shown in Figure 2. **B:** Third CAST/Ei injured spinal cord. Arrows identify retrogradely labeled axons from the PNS. Asterisk indicates the sight of injury.

Suppl Figure 4: Dorsal column injury longest axon quantification (Related to Figure 3)**:** Preconditioned CAST show significant axonal growth with the dorsal column injury compared with C57. Mean ± SEM. (**p<0.01, 2184.9 (557.1) CI 826.3-3543.6; two-way ANOVA, post-hoc Sidak's).

Suppl Figure 5: RAG gene regulation between C57 and CAST DRGs (Related to - *Genome-wide expression profiling of naïve and preconditioned DRGs across all nine strains* - in Results)**:** Comparison of the regulation following preconditioning injury of known regeneration associated genes (RAGs) between C57BL/6 (blue) and CAST/Ei (red) showing little to no difference in most of these genes.

Suppl Figure 6: Immunohistochemistry and *in situ* hybridization of Activin cascade members (Related to - *Activin signaling components in C57 and CAST DRGs* - in Results)**:** Expression of Inhba mRNA; Activin-β_A immunoreactivity; Acvr1a mRNA; Acvr2a immunoreactivity; Acvr2b mRNA; pSmad2/3 immunoreactivity in preconditioned CAST/Ei and C57BL/6 DRG neurons respectively. Scale, 100 µm.

Suppl Figure 7: *In vitro* gain of function assay using rat RGC cells (Related to - *Activin gain- and loss-of-function* - in Results)**:** Rat retinal ganglion cells subject to preconditioning with optic nerve crush

and low dose zymosan (6.4µg/retina, 3 days prior to culture) demonstrate significantly more growth in the presence of Activin-A, Activin-B and Activin-AB peptides. Statistical analysis: Student's t-test, two-tailed. ** $p<0.01$.

Supplemental Tables:

Suppl Table 1 (Related to Figure 1)

Growth of DRG neurons from nine inbred mouse strains on myelin (ppt)

Suppl Table 2 (Related to - *Heritability estimates of axonal growth phenotype* - in Results)

Narrow-sense heritability estimates h^2 (ppt)

Suppl Table 3 (Related to - *Genome-wide expression profiling of naïve and preconditioned DRGs across all nine strains* - in Results)

Full microarray DRG screen data set across 9 mice strains (xls)

Suppl Table 4 (Related to - *Genome-wide expression profiling of naïve and preconditioned DRGs across all nine strains* - in Results)

Pearson correlation between DRG gene expression and DRG axonal growth across 9 mice strains (xls)

Suppl Table 5 (Related to - *Genome-wide expression profiling of naïve and preconditioned DRGs across all nine strains* - in Results)

WGCNA analysis of microarray data set with cross comparison to rat conditioning response (xls)

References

Clarkson, A.N., Lopez-Valdes, H.E., Overman, J.J., Charles, A.C., Brennan, K.C., and Thomas Carmichael, S. (2013). Multimodal examination of structural and functional remapping in the mouse photothrombotic stroke model. J Cereb Blood Flow Metab 33, 716-723.

Griffin, R.S., Costigan, M., Brenner, G.J., Ma, C.H., Scholz, J., Moss, A., Allchorne, A.J., Stahl, G.L., and Woolf, C.J. (2007). Complement induction in spinal cord microglia results in anaphylatoxin C5a-mediated pain hypersensitivity. J Neurosci 27, 8699-8708.

Li, S., Overman, J.J., Katsman, D., Kozlov, S.V., Donnelly, C.J., Twiss, J.L., Giger, R.J., Coppola, G., Geschwind, D.H., and Carmichael, S.T. (2010). An age-related sprouting transcriptome provides molecular control of axonal sprouting after stroke. Nat Neurosci 13, 1496-1504.

Ma, C.H., Omura, T., Cobos, E.J., Latremoliere, A., Ghasemlou, N., Brenner, G.J., van Veen, E., Barrett, L., Sawada, T., Gao, F.*, et al.* (2011). Accelerating axonal growth promotes motor recovery after peripheral nerve injury in mice. J Clin Invest 121, 4332-4347.

Overman, J.J., Clarkson, A.N., Wanner, I.B., Overman, W.T., Eckstein, I., Maguire, J.L., Dinov, I.D., Toga, A.W., and Carmichael, S.T. (2012). A role for ephrin-A5 in axonal sprouting, recovery, and activity-dependent plasticity after stroke. Proc Natl Acad Sci U S A 109, E2230-2239.

Puttagunta, R., Tedeschi, A., Soria, M.G., Hervera, A., Lindner, R., Rathore, K.I., Gaub, P., Joshi, Y., Nguyen, T., Schmandke, A.*, et al.* (2014). PCAF-dependent epigenetic changes promote axonal regeneration in the central nervous system. Nat Commun 5, 3527.

Yin, Y., Cui, Q., Li, Y., Irwin, N., Fischer, D., Harvey, A.R., and Benowitz, L.I. (2003). Macrophage-derived factors stimulate optic nerve regeneration. J Neurosci 23, 2284-2293.

Yin, Y., Henzl, M.T., Lorber, B., Nakazawa, T., Thomas, T.T., Jiang, F., Langer, R., and Benowitz, L.I. (2006). Oncomodulin is a macrophage-derived signal for axon regeneration in retinal ganglion cells. Nat Neurosci 9, 843-852.

Supplemental Fig. 1

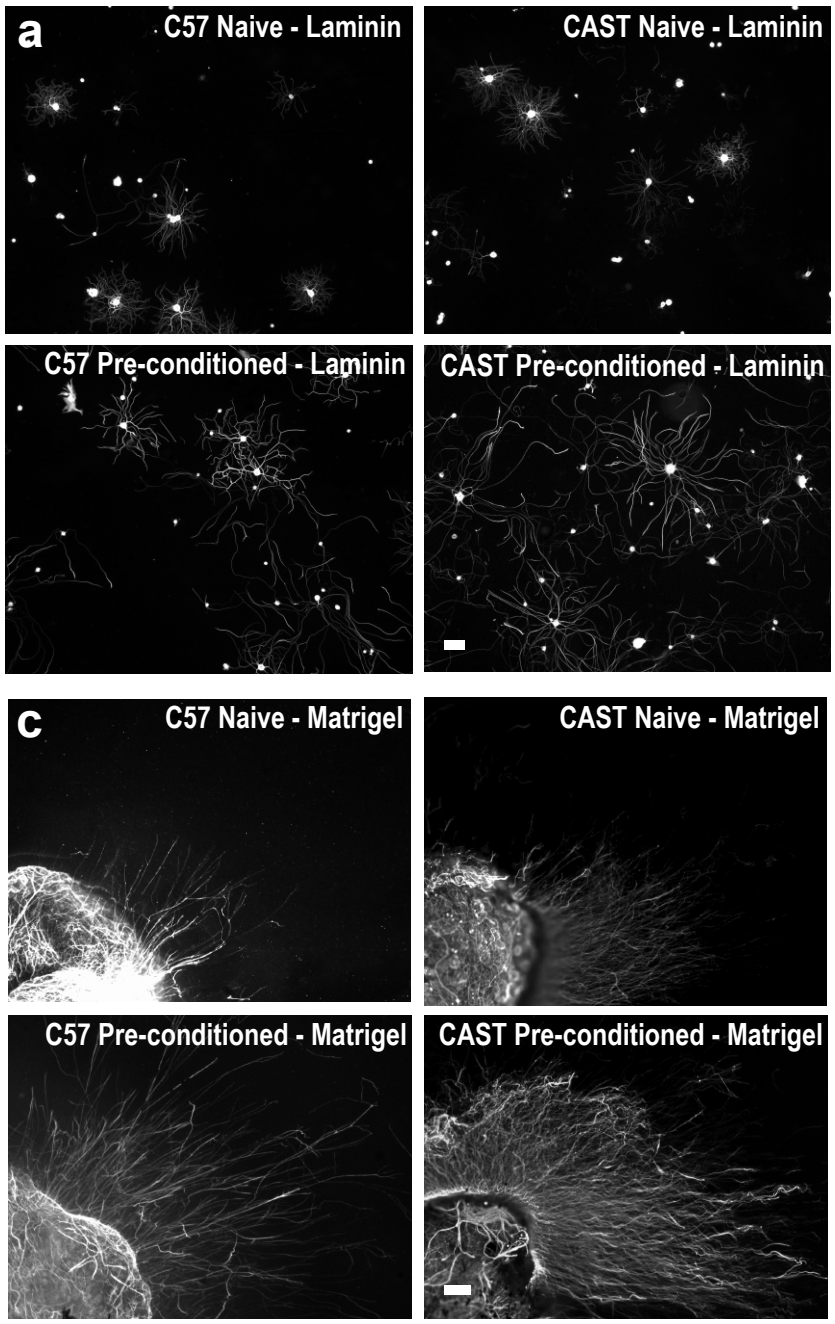

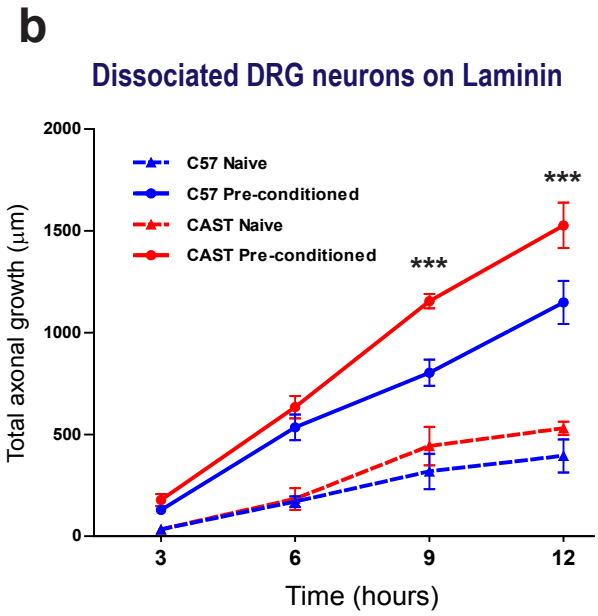

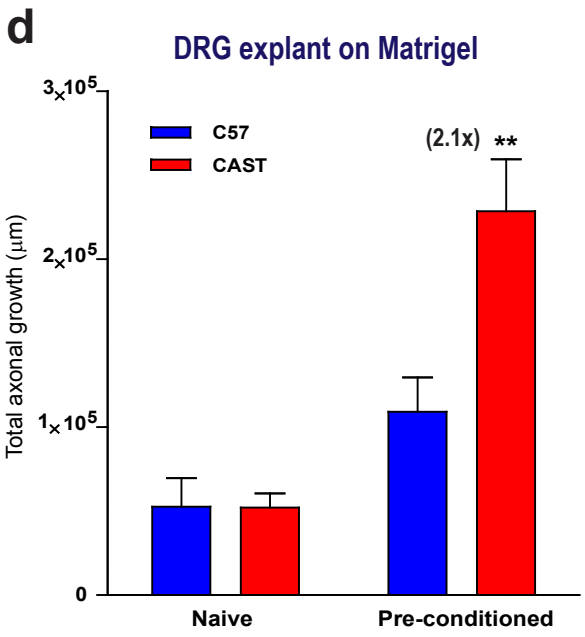

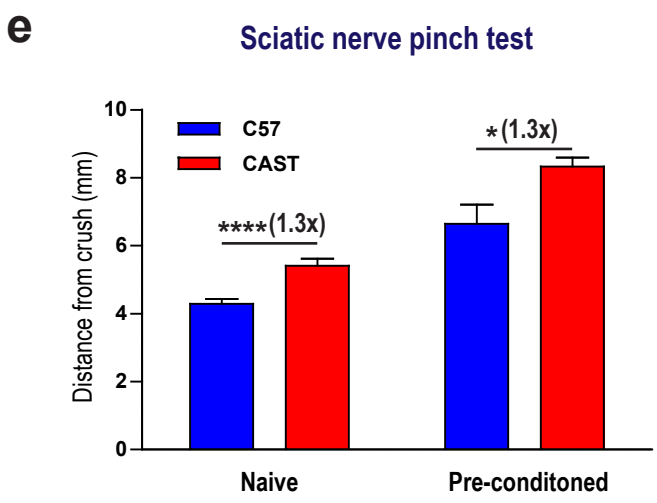

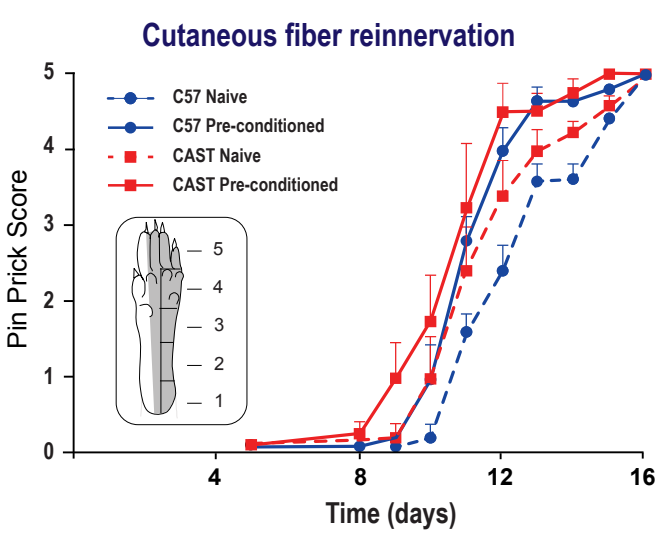

a C57BL/6 Animal Two: Pre-conditioned injured spinal cord

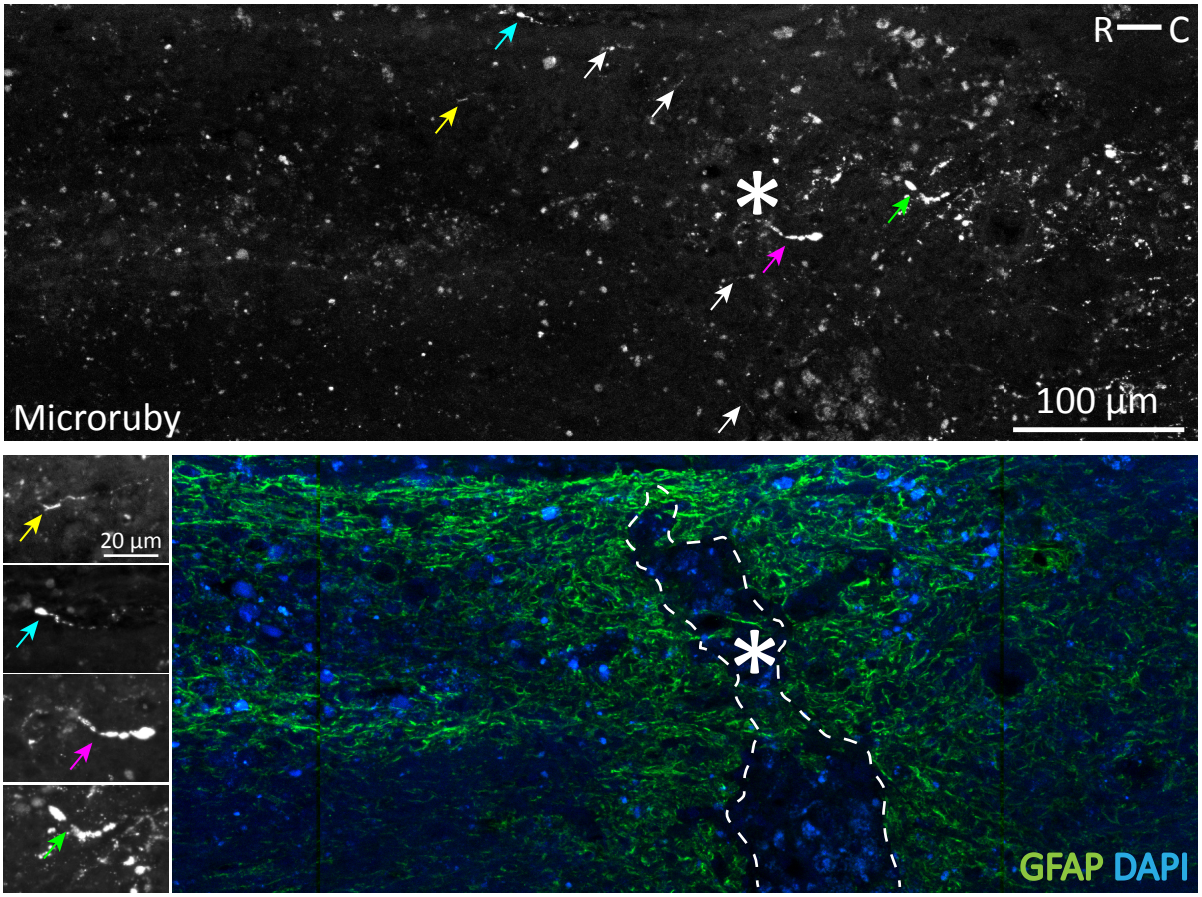

b C57BL/6 Animal Three: Pre-conditioned injured spinal cord

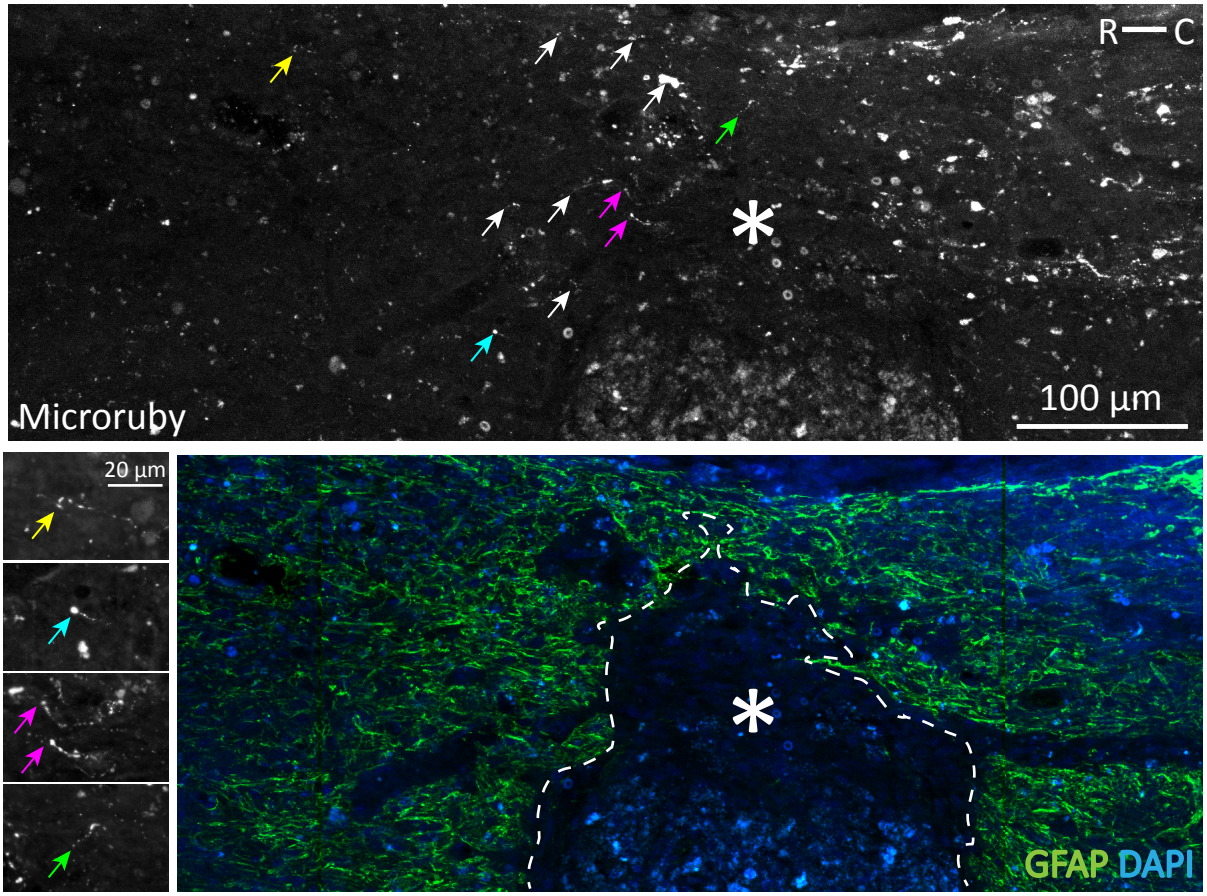

a CAST/Ei Animal Two: Pre-conditioned injured spinal cord

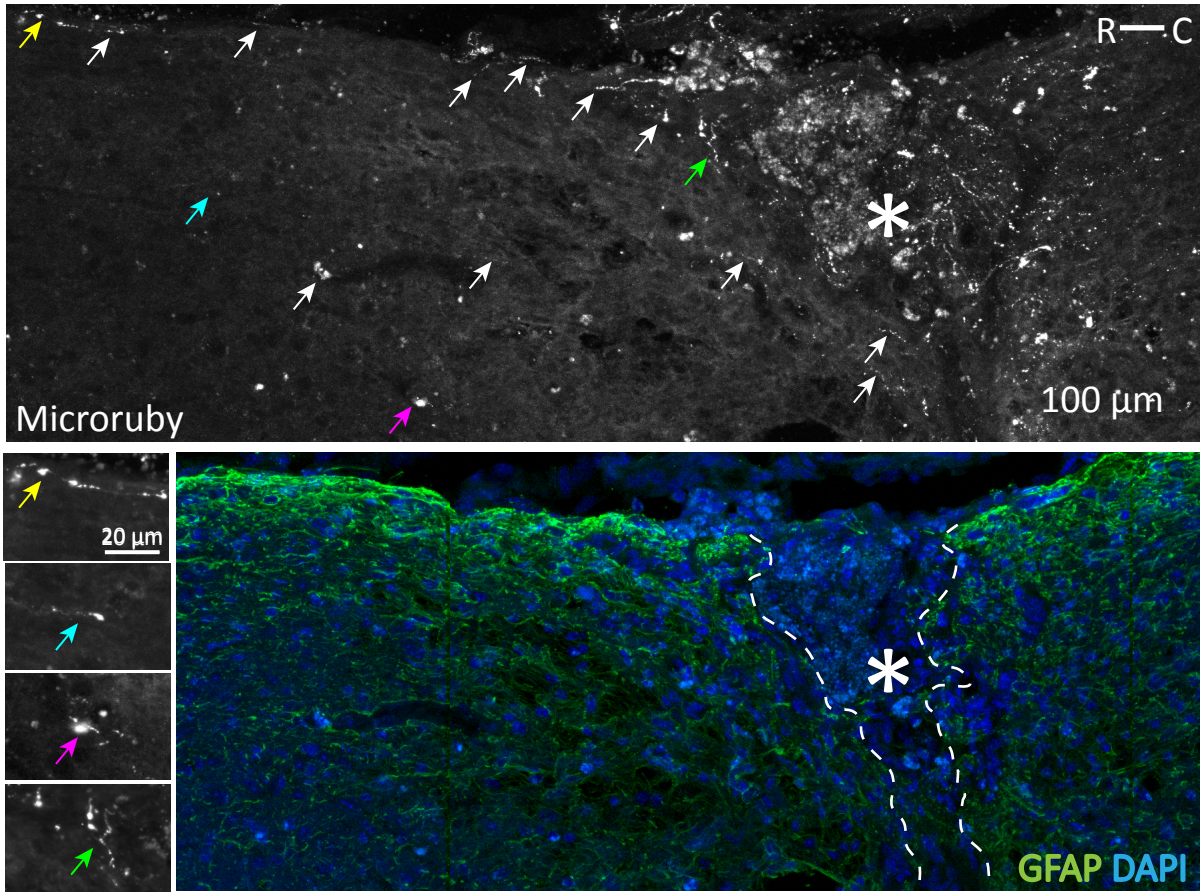

b CAST/Ei Animal Two: Pre-conditioned injured spinal cord

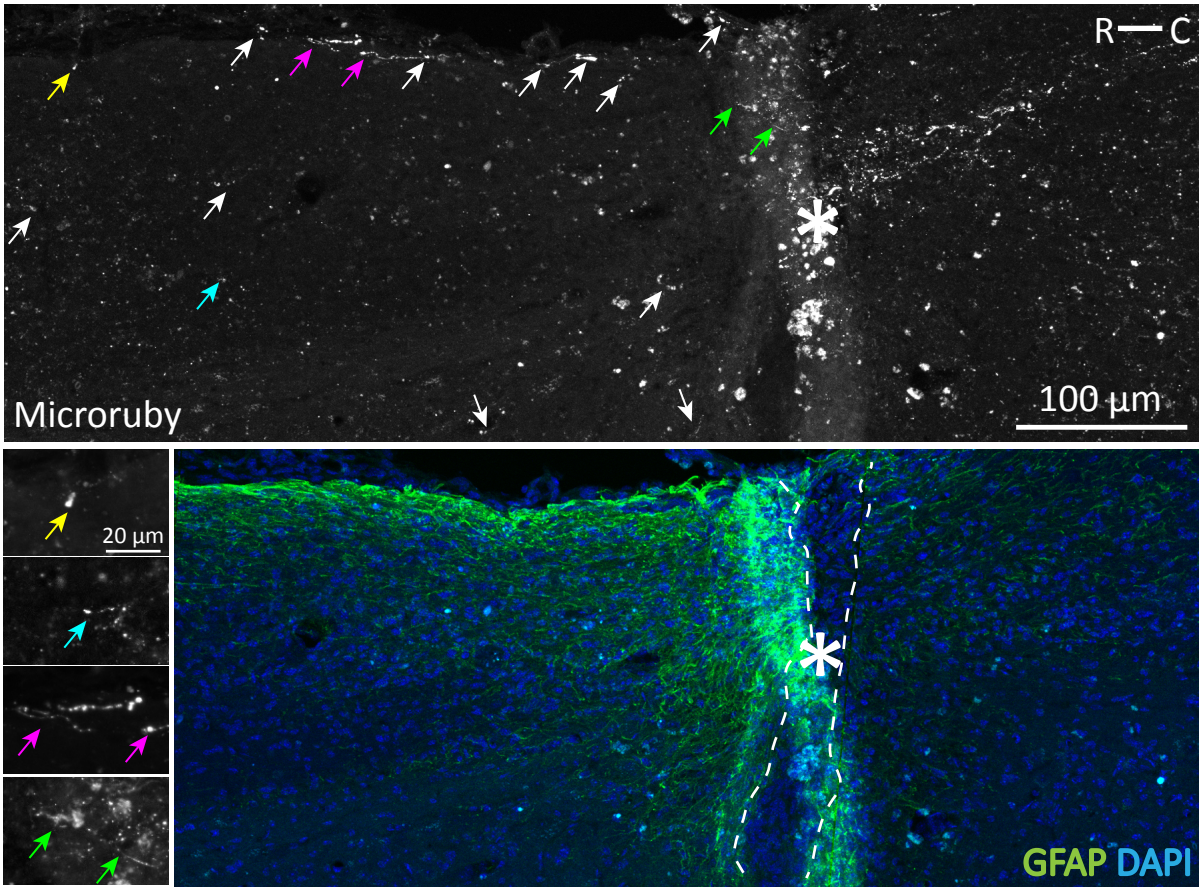

Supplemental Fig. 4

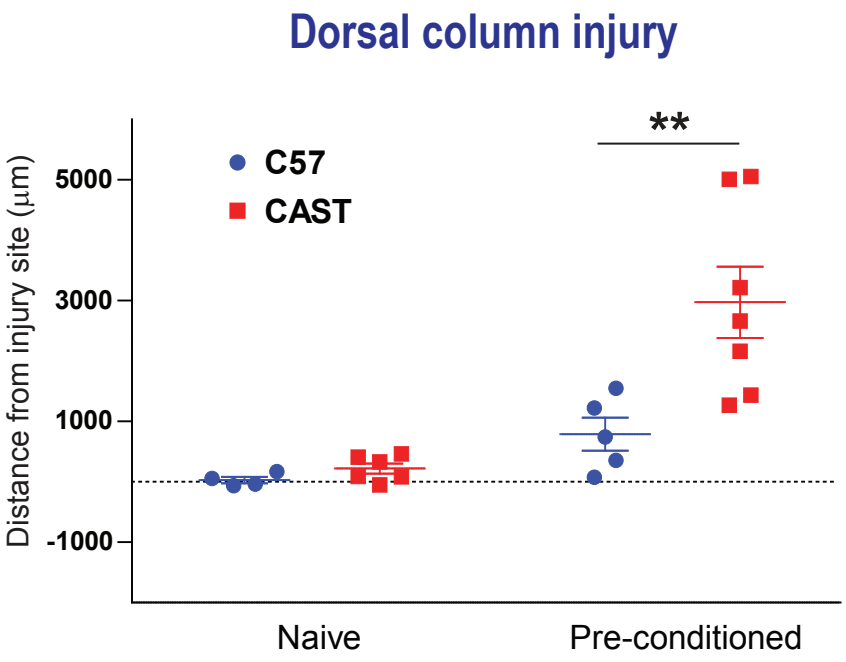

Supplemental Fig. 5

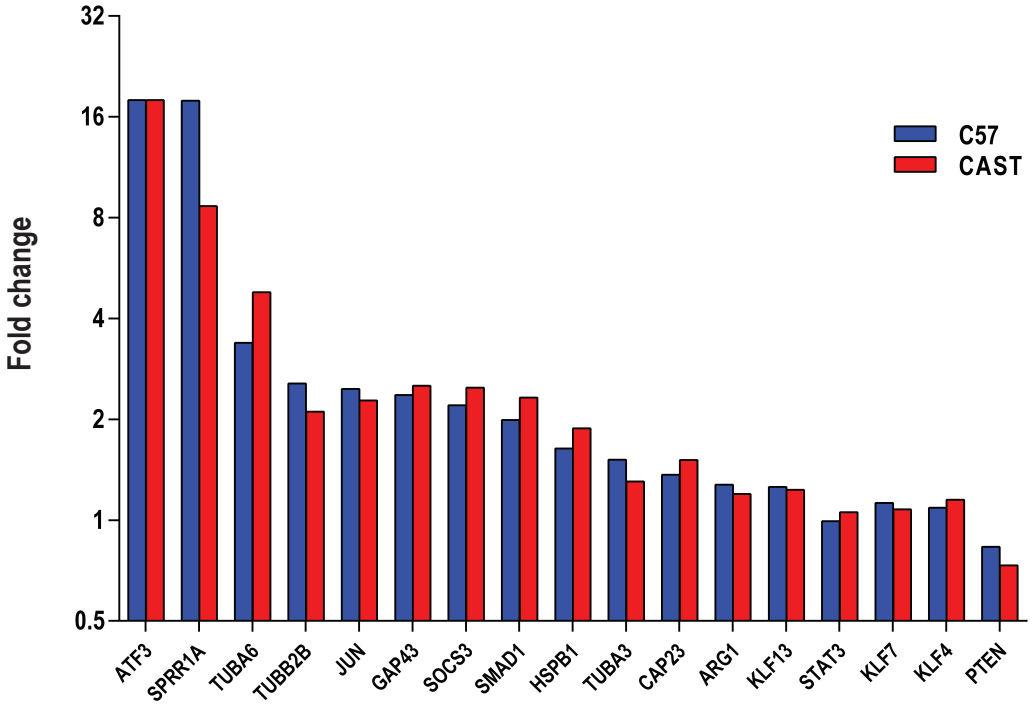

Supplemental Fig. 6

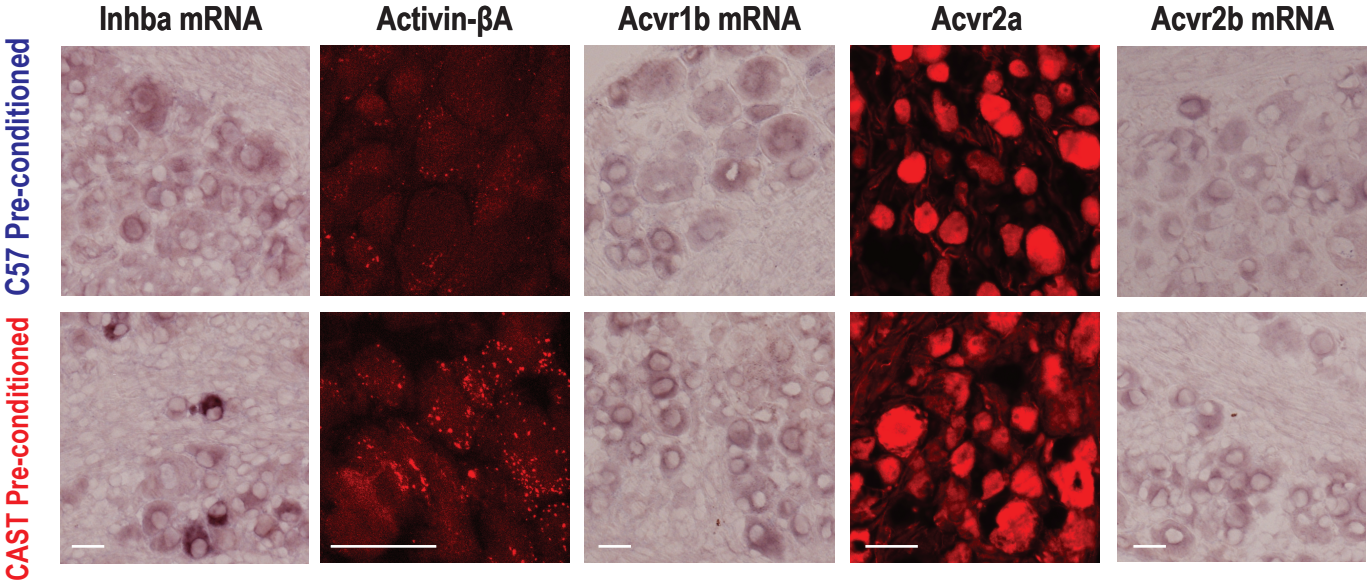

Supplemental Fig. 7

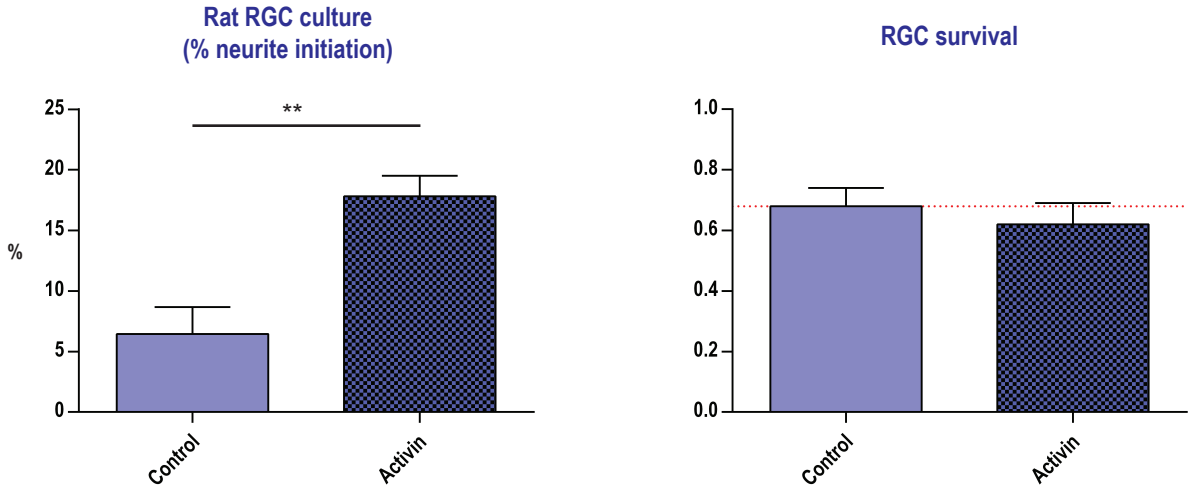

Supp Table 1

	C57	129	WSB	A/J	NOD	C3H	DBA	NZO	CAST	CAST / (other strains)
Naïve Sprouting (%)	**0.4** ±0.2	**1.7** ±0.7	**0.7** ±0.2	**2** ±0.4	**0.9** ±0.5	**0.7** ±0.1	**0.9** ±0.2	**1.6** ±0.4	**4.2** ±0.6	3.6 x
Naïve Axon Length (μm)	**22** ±3	**43** ±4	**28** ±1.2	**40** ±3	**37** ±4	**26** ±2	**34** ±5	**45** ±2	**67** ±8	2 x
Preconditioned Sprouting (%)	**2.5** ±0.4	**7.8** ±2.9	**8** ±0.9	**9.2** ±1.2	**9.8** ±2.1	**10.6** ±0.9	**11** ±1	**13** ±2.1	**50.3** ±1.8	5.5 x
Preconditioned Axon Length (μm)	**44** ±3	**77** ±5	**74** ±4	**88** ±10	**84** ±8	**115** ±5	**97** ±8	**126** ±11	**306** ±18	3.5 x
Ratio Sprouting (Precond/Naïve)	6.6 x	11.8 x	11.4 x	9.8 x	6.9 x	6.5 x	6.3 x	7.0 x	11.9 x	
Ratio Axon Length (Precond/Naïve)	2.0 x	3.0 x	2.7 x	2.6 x	2.3 x	2.9 x	2.2 x	2.8 x	4.6 x	

Supplemental Table 1: Growth of DRG neurons from nine inbred mouse strains on myelin

Supp Table 2

Naïve DRG - Normalized	N	Range	Range Norm	F-value	P-value	h^2	#EF
Inhibitory Growth (Sprouting %)	52	7.2	4.67	6.56	1.56E-05	0.31	3.82
Inhibitory Growth (Axon Length µm)	50	96.5	4.64	8.69	8.73E-07	0.41	3.40
Preconditioned DRG - Normalized							
Inhibitory Growth (Sprouting %)	50	56.9	4.64	13.5	3.17E-09	0.54	3.84
Inhibitory Growth (Axon Length µm)	50	345.9	4.64	29.3	2.15E-14	0.72	3.23

Supplemental Table 2: Narrow-sense heritability estimates h^2 of DRG neuron growth on myelin. N is sample size. Range Norm is the range of the phenotype normalized by an inverse normal transform. Heritability estimates for inbred strains are calculated by h2 = (σ_G2/2) / ((σ_G2/2)+σ_E2). #EF are the number of likely heritable factors effecting each trait. #EF is calculated by #EF = (largest strain mean-smallest strain mean)2 /(4 x VA). P-values and F-values are both obtained through ANOVA.

Click here to download Supplemental Movies & Spreadsheets: Suppl Table 3 (Full data set_Arrays)lite-v2.xlsx

Click here to download Supplemental Movies & Spreadsheets: Suppl Table 4 (Pearson_Inhibitory growth).xlsx

Click here to download Supplemental Movies & Spreadsheets: Suppl Table 5 (Mouse and Rat PNS injury overlap).xlsx